RSC Advances

PAPER

View Article Online
View Journal | View Issue

Cite this: *RSC Adv.*, 2018, **8**, 4354

Electronic and steric effects of substituents in 1,3-diphenylprop-2-yn-1-one during its reaction with $Ru_3(CO)_{12}$†

Lei Xu, Shasha Li, Liping Jiang, Guofang Zhang,* Weiqiang Zhang and Ziwei Gao

Thermal reaction of $Ru_3(CO)_{12}$ with alkynyl ketones PhC≡CC(O)R (R=Ph (**1**); 2-Cl-Ph (**2**); 4-NO_2-Ph (**3**); 2-NH_2-Ph (**4**); and 2-CH_3COO-Ph (**5**)) proceeds in toluene with the formation of $Ru_3(CO)_9(\mu\text{-}CO)(\eta^4$-triruthenium) derivatives (**1a–5a**), $Ru(CO)_3(\eta^4$-ruthenole) derivatives (**1b–4b**, **1c–5c** and **4d**) and cyclotrimerization products (**1e–2e** and **1f–3f**). Compounds **1a–5a** were isolated from the reaction of $Ru_3(CO)_{12}$ with one equivalent of **1–5**, respectively. Ruthenoles **1b–3b** and **1c–3c** were collected by adding **1–3** to the corresponding **1a–3a** in a molar ratio of 1 : 1. Cyclotrimerization products **1e–2e** and **1f–3f** were obtained when **1–3** were added to their corresponding **1b–2b** and **1c–3c**, respectively. **4b**, **4c** and **4d** were afforded during the reaction of **4** with **4a**, but only **5c** was collected during the reaction of **5** with **5a**. All compounds were characterized by NMR, FT-IR, and MS-ESI and most of them were structurally confirmed by single crystal X-ray diffraction. The results suggest that electronic and steric effects of the substituents in the phenyl ring of 1,3-diphenylprop-2-yn-1-one play important roles in regulating the reaction pathways. An electron-withdrawing group is beneficial to the formation of **b**, **c** and further formation of **e** and **f**; an electron-donating group favors the production of ruthenoles **b**, **c** and **d**, but disfavors the formation of **e** and **f**; a substituent with large steric-hindrance prefers only the formation of **c**.

Received 25th December 2017
Accepted 15th January 2018

DOI: 10.1039/c7ra13626a

rsc.li/rsc-advances

Introduction

$Ru_3(CO)_{12}$ has attracted the great interest of researchers in inorganic, organic and catalytic chemistry due to its abundant reactivity and unique catalytic activity.[1] It has been highly effective in the activation and conversion of chemical bonds in the construction of diverse C–X (X = C, N, O, Si, *etc.*) bonds,[2] and widely used in reactions such as hydroamination,[3] hydroesterification,[4] silylation,[5] cycloaddition,[6] transfer hydrogenation,[7] carbonylation[8] and hydrohydroxyalkylation.[9] In order to understand the mechanisms of $Ru_3(CO)_{12}$ activated C–C and C–H bonds, reactions of $Ru_3(CO)_{12}$ with NHCs, arenes, alkenes and alkynes were extensively investigated.[10] Some carbonyl ruthenium compounds formed *via* $Ru_3(CO)_{12}$ and unsaturated hydrocarbons have been used in catalytic systems.[11] In these reactions, coordination atoms play a very important role in the activation of neighboring chemical bonds and construction of compound skeletons,[12] such as the interaction between oxygen atoms and ruthenium atoms in the activation of open-cage fullerenes with ruthenium carbonyl clusters.[13] These conclusions provide more possibilities for $Ru_3(CO)_{12}$ to become a potential catalyst for the conversion of alkyne compounds.

The reactions of $Ru_3(CO)_{12}$ with alkynes have been studied for many years. A variety of coordination modes were reported.[14] There are usually relevant to many catalytic processes involving polynuclear species and unsaturated organic molecules.[15] In 2005, compound $(\mu\text{-}H)_2Ru_3(CO)_9\{\mu_3\text{-}\eta^2[H_2C{=}C(H)C{\equiv}CC(=O)OCH_3]\}$ was isolated by the activation of methanol and CO in the reaction of 1,4-dichloro-but-2-yne (DCB) and $Ru_3(CO)_{12}$.[16] Then, two types of complexes $Ru_3(CO)_9(\mu\text{-}CO)\{\mu_3\text{-}\eta^2\text{-}(\|)\text{-}HC{\equiv}CR\}$ and $Ru_3(CO)_9(\mu\text{-}CO)\{\mu_3\text{-}\eta^2\text{-}(\perp)\text{-}HC{\equiv}CR\}$(R=$C_6H_4$-4-$CH_3$, C_6H_3-2,5-$(CH_3)_2$, *etc.*) were collected by M. Hernandez-Sandoval in the reaction of activated cluster $[Ru_3(CO)_{10}(NCMe_3)_2]$ with terminal alkynes.[17] Recently, P. Mathur demonstrated that one C≡C bond of FcC_2C_2Ph (Fc = ferrocenyl) was activated by $Ru_3(CO)_{12}$, and a series of novel mixed Ru/Pt clusters were isolated.[18] In general, the reaction of $Ru_3(CO)_{12}$ with functionalized acetylenes can afford a variety of unexpected products,[19] that means alkyne ligands always experienced sophisticated transformations, these properties limited our understanding on activation of C≡C bonds.

Key Laboratory of Applied Surface and Colloid Chemistry, MOE/School of Chemistry and Chemical Engineering, Shaanxi Normal University, Xi'an 710062, China. E-mail: gfzhang@snnu.edu.cn

† Electronic supplementary information (ESI) available: Crystal structures of **1a**, **1f**, **2a**, **3b**, **4b**, **5c**, **2f**, **3c** and **1c**, CIF; checkcif, ^{1}H NMR spectra, $^{13}C\{1H\}$ NMR spectra, FT-IR spectra and other electronic format. CCDC 1553521, 1553523, 1553526, 1553527, 1553511, 1553512, 1545197, 1545199, 1553513, 1553516, 1553504 and 1553509. For ESI and crystallographic data in CIF or other electronic format see DOI: 10.1039/c7ra13626a

Alkynyl ketones are important structural units with unsaturated functional groups. They are often employed as key templates in modern chemical synthesis.[20] The C≡C bonds of ynones are good π-acceptors,[21] whilst the adjacent carbonyl groups can coordinate as 2e σ donors.[22] For understanding the reactive activity of 1,3-ynones with $Ru_3(CO)_{12}$, thermolytic reaction of $Ru_3(CO)_{12}$ with 1-(4-methoxyphenyl)-3-phenylprop-2-yn-1-one have been investigated systematically in our group, and a series of Ru_2–Ru_4 framework clusters including a triruthenium and a tetraruthenium intermediates and three ruthenoles were isolated.[23] After a detailed analysis of the results, we proposed that the electron-donating methoxy group in the phenyl ring of the 1-(4-methoxyphenyl)-2-propyn-1-one may play an important role in the transformation reaction. As a continuing work in the chemistry of $Ru_3(CO)_{12}$ with alkynyl ketones, we investigated the electronic and steric effects of the substituents in the phenyl ring of 1,3-diphenylprop-2-yn-1-one on the structures of the intermediates and final products during its thermolytic reactions with $Ru_3(CO)_{12}$.

In this paper, we examined in detail the reaction process of $Ru_3(CO)_{12}$ with 1,3-diphenylprop-2-yn-1-one derivatives (**1–5**) containing in its phenyl ring, for example, no substituent (**1**), electron-withdrawing groups (**2–3**), an electron-donating group (**4**) and a sterically hindered group (**5**). The coordination and coupling of the alkynyl ketone molecules formed a series of intermediate ruthenium clusters and cyclotrimerization products. Through a detailed examination of the reaction processes, we revealed that substituents in the phenyl rings of the acetylenic ketones are vital for the reaction process and that the formation of products has been affected comprehensively by the steric hindrance and/or electronic properties of the substituents.

Results and discussion

Syntheses and characterization

Reactions of $Ru_3(CO)_{12}$ and the 1,3-ynones were performed in toluene at 90 °C under nitrogen atmosphere and monitored consistently by TLC technique. It was found that color of each reaction solution gradually changed from orange to red-brown and the non-reacted $Ru_3(CO)_{12}$ precipitated after cooling. All isolated compounds were completely characterized by FT-IR, NMR, ESI mass spectrometry and most of them were additionally characterized by single crystal X-ray diffraction. The reaction process is illustrated in Scheme 1 according to the experimental results and TLC technique as well as the structural characterization analyses.

Synthesis of $Ru_3(CO)_9(\mu\text{-}CO)(\eta^4\text{-triruthenium})$ derivatives 1a–5a

When a toluene solution of an 1,3-ynone (**1–5**) (0.03 mmol) and $Ru_3(CO)_{12}$ (0.01 mmol) was stirred at 90 °C for 30 min under nitrogen atmosphere, $Ru_3(CO)_9(\mu\text{-}CO)(\eta^4\text{-triruthenium})$ derivatives (**1a–5a**) were formed due to binding of the C≡C bonds of **1–5** and the Ru metal skeletons. Each of the new clusters has a similar structural framework according to the characterization results and the crystal structure of **5a** is shown in Fig. 1 was taken as an example. The IR spectrum of **5a** was similar to those

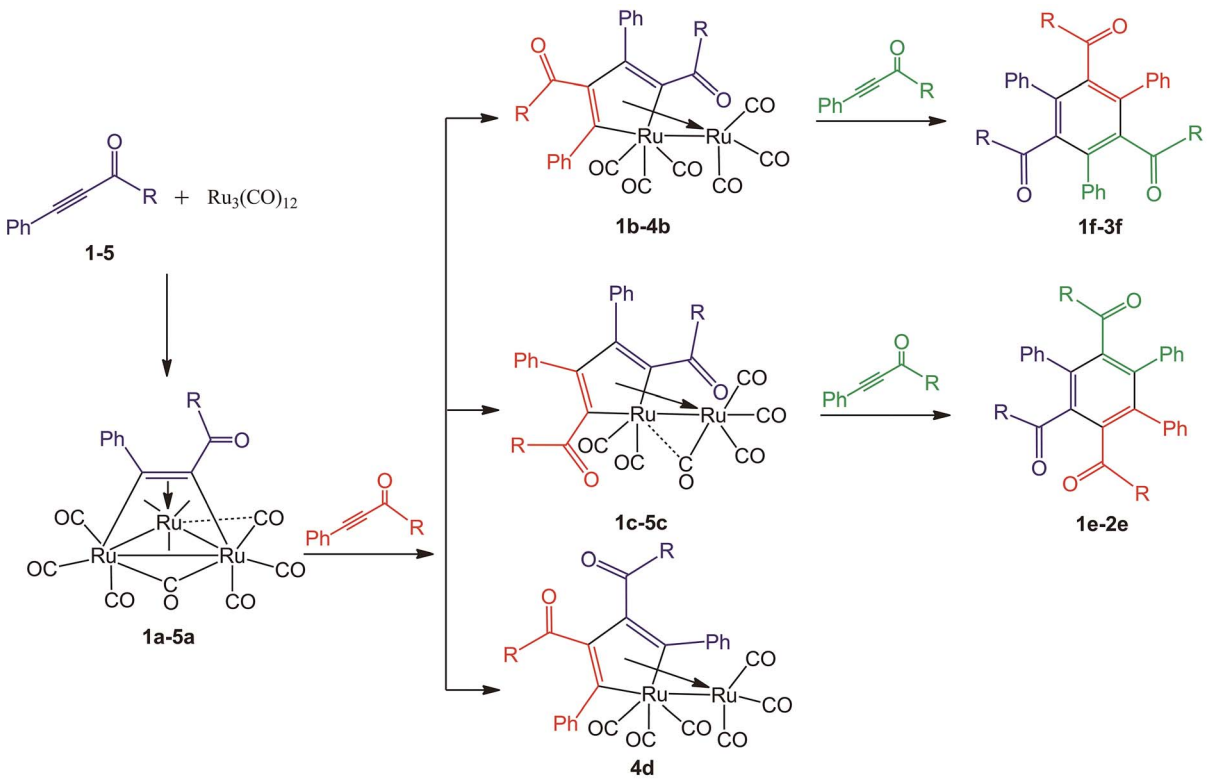

Scheme 1 The reaction process of $Ru_3(CO)_{12}$ with 1,3-ynones (**1–5**). R=Ph (**1**); 2-Cl-Ph (**2**); 4-NO_2-Ph (**3**); 2-NH_2-Ph (**4**); 2-CH_3COO-Ph (**5**).

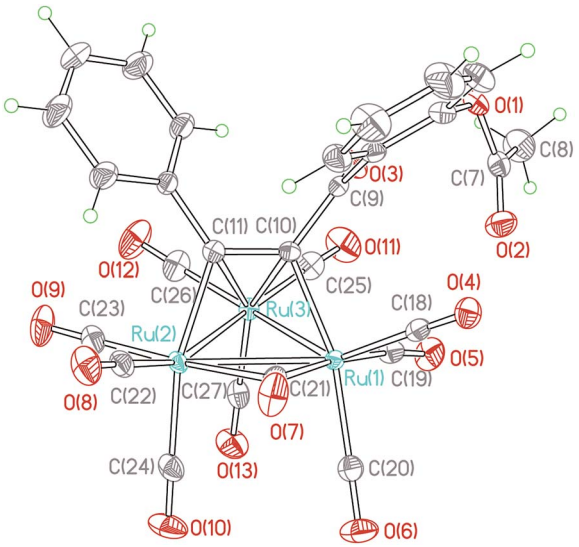

Fig. 1 ORTEP view of cluster **5a** showing 50% ellipsoids. Selected bond lengths (Å) and bond angles (°): Ru1–Ru2 = 2.845(2); Ru2–Ru3 = 2.712(2); Ru1–Ru3 = 2.749(2); Ru1–C19 = 1.939(3); Ru1–C21 = 2.029(2); Ru1–C10 = 2.126(2); Ru2–C11 = 2.091(2); Ru2–C21 = 2.337(2); Ru3–C11 = 2.317(2); Ru3–C10 = 2.211(2); Ru3–C19 = 2.873(2); C10–C11 = 1.396(3); C9–C10 = 1.498(3); C9–O3 = 1.219(2); C19–O5 = 1.337(3); C21–O7 = 1.149(3); Ru1–C19–Ru3 = 66.4(1); Ru1–C21–Ru2 = 81.0(1).

observed in the compounds $M_3(CO)_9(\mu\text{-}CO)L$ (M = Ru, Os).[23,24] The absorption bands peaked in the range of 2017–2104 cm^{-1} and at 1878 cm^{-1} were assigned to the terminal and bridging CO groups, respectively. The dramatic red shift of the stretch vibration of the C≡C bond in **5a** from 2191 cm^{-1} to *ca.* 1446 cm^{-1} reveals further that the coordination interaction between the carbon atoms of the C≡C bond and the Ru central metals is very strong. The chemical shifts of the C≡C bond moved downwards to 150.8 and 148.2 ppm, confirming again the strong interaction between the C≡C bond and the Ru atoms. The chemical shifts of the carbonyl carbon atoms directly with Ru atoms cannot be distinguished, indicating that in solution there are fluxional for the terminal and bridging CO on the $^{13}C\{1H\}$ NMR time scale.

The compound **5a** consists of a triangular arrangement of the ruthenium atoms, in which the Ru–Ru bond distances are in the range of 2.712(2)–2.845(2) Å. The coordination of the alkynyl ketone (**5**) with Ru3 is in a η^2 mode, but with Ru1 and Ru2 is in a η^1 mode. The C10–C11 bond length is 1.396(3) Å, located between the typical C–C single bond and double bond, indicative again of the strong coordination strength of the Ru–C bonds.[25] The distances of Ru1–C19 and Ru3–C19 are 1.939(3) and 2.873(2) Å, respectively. The angle of Ru1–C19–O5 is 169.2(2)°. In addition, there is a carbonyl exists between Ru1 and Ru3 atoms.

Synthesis of $Ru(CO)_3(\eta^4$-ruthenole) derivatives 1b–4b, 1c–5c and 4d

When the reaction time of the above reaction was prolonged from 0.5 h to 1 h, $Ru(CO)_3(\eta^4$-ruthenole) derivatives **b** (**1b–4b**), **c** (**1c–5c**) and **d** (**4d**) were separated by flash chromatography. The structural characterizations showed that structures of the new ruthenoles are of diverse coupling combinations of the C≡C units in the 1,3-ynones, such as modes **b** (head to tail coupling), **c** (head to head coupling) and **d** (tail to tail coupling).[23] Each ruthenole contains a metallacyclopentadienyl framework, which is alike in structure to the carbonyl complexes $[M(CO)(\eta^4$-metallole)] (M = Fe, Ru, Os) formed by combination of alkynes with group 8 metals.[23,26] The molecular structure of **1b**, as an example, was depicted in Fig. 2. The structure of **1b** showed an eclipsed conformation of the carbonyls on the two ruthenium centers, with the dihedral angle of R1–Ru2–$C35_{plane}$ and R1–Ru2–$C32_{plane}$ being 2.1(1)°. The special arrangement geometrically prevents an apical carbonyl to be close enough to the ring metal Ru1 for a CO bridging conformation. Hence, all carbonyls are terminal with almost parallel Ru–C–O angle.

Compared the structures of **b** and **c**, each of the crystal structures of ruthenoles **c** (taking **2c**·$1/2C_6H_{14}$ shown in Fig. 3 as an example) appeared a routine staggered conformation of the carbonyls. The dihedral angles between Ru1–Ru2–$C35_{plane}$ and Ru1–Ru2–$C31_{plane}$, Ru1–Ru2–$C32_{plane}$ are 58.4(2)° and 41.0(2)°, respectively. The distances of Ru1–C35 is 2.742(5) Å. The staggered orientation in **2c**·$1/2C_6H_{14}$ allows the C35 close to the Ru1 metal for a weak interaction, which formed a semi-bridging carbonyl across the Ru–Ru bond. The IR absorption at 1944 cm^{-1} also confirms its presence.

The crystal structure of **4d**·$3/4CH_2Cl_2$ (Fig. 4) also showed an eclipsed conformation of carbonyls on the two ruthenium centers, the dihedral angle of R1–Ru2–$C35_{plane}$ and R1–Ru2–$C33_{plane}$ is 1.0(1)° between the equatorial Ru2–CO and Ru1–CO bonds, indicating that the Ru1, Ru2, C33 and C35 atoms are almost coplanar. All carbonyls are terminal with almost linear Ru–C–O angle, similar to those in compounds **1b–4b**.

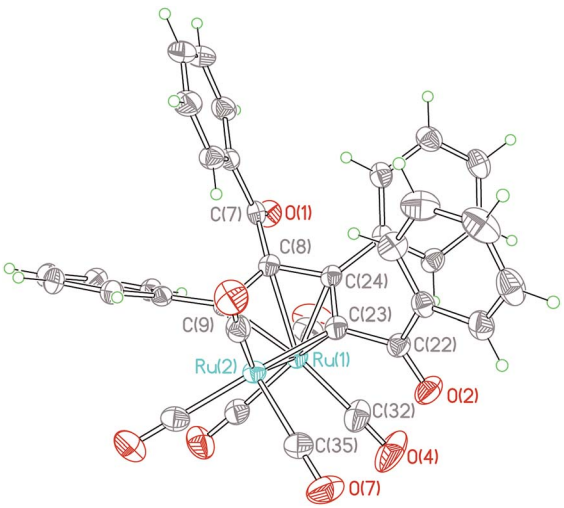

Fig. 2 ORTEP view of cluster **1b** showing 50% ellipsoids. Selected bond lengths (Å) and bond angles (°): Ru1–Ru2 = 2.734(2), Ru1–C8 = 2.254(2), Ru1–C9 = 2.316(2), Ru1–C24 = 2.243(2), Ru1–C23 = 2.252(2), Ru2–C9 = 2.098(2), Ru2–C23 = 2.068(2), C7–C8 = 1.515(3), C7–O1 = 1.214(2), C8–C9 = 1.411(3), C8–C24 = 1.458(3), C23–C24 = 1.420(3), C22–C23 = 1.491(3), C22–O2 = 1.217(2), C9–Ru2–C23 = 77.6(1), Ru1–C32–O4 = 177.0(2), Ru2–C35–O7 = 179.6(2).

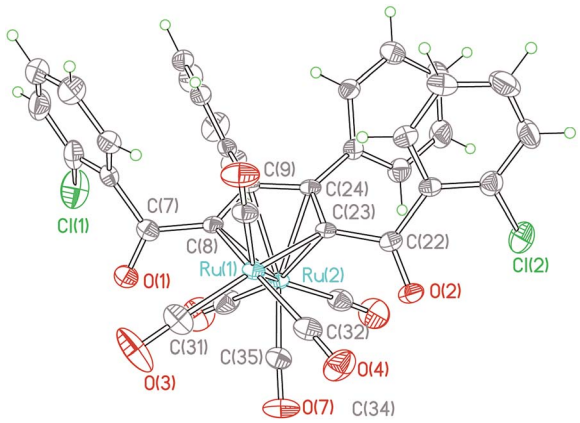

Fig. 3 ORTEP view of cluster **2c**·1/2C_6H_{14} showing 50% ellipsoids (solvent molecules have been omitted for clarity). Selected bond lengths (Å) and bond angles (°): Ru1–Ru2 = 2.712(1), Ru1–C8 = 2.097(4), Ru1–C23 = 2.096(5), Ru1–C35 = 2.742(5), Ru2–C8 = 2.223(4), Ru2–C9 = 2.300(5), Ru2–C23 = 2.232(5), Ru2–C24 = 2.310(5), Ru2–C35 = 1.908(5), C7–C8 = 1.496(7), C7–O1 = 1.213(7), C8–C9 = 1.436(6), C9–C24 = 1.435(7), C23–C24 = 1.440(5), C22–C23 = 1.495(7), C22–O2 = 1.215(5), C8–Ru1–C23 = 53.2(1), Ru2–C35–O7 = 169.7(4), Ru2–C35–Ru1 = 68.7(1).

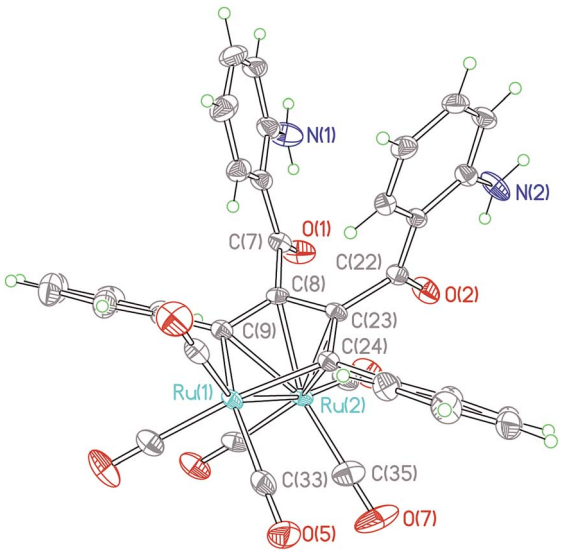

Fig. 4 ORTEP view of cluster **4d**·3/4CH_2Cl_2 showing 50% ellipsoids (solvent molecules have been omitted for clarity). Selected bond lengths (Å) and bond angles (°): Ru1–Ru2 = 2.704(4), Ru1–C9 = 2.085(3), Ru1–C24 = 2.083(3), Ru2–C9 = 2.319(4), Ru2–C8 = 2.224(3), Ru2–C23 = 2.234(2), Ru2–C24 = 2.339(3), C7–C8 = 1.518(5), C7–O1 = 1.227(5), C8–C9 = 1.417(5), C8–C23 = 1.460(5), C23–C24 = 1.412(5), C22–C23 = 1.523(5), C22–O2 = 1.233(5), C9–Ru1–C24 = 79.2(1), Ru1–C33–O5 = 176.9(3), Ru2–C35–O7 = 174.8(4).

Synthesis of the cyclotrimerization products e (1e–2e) and f (1f–3f)

When $Ru_3(CO)_{12}$ (0.1 mmol) reacted with **3** equivalent of an 1,3-ynone (**1–3**) (0.3 mmol) in toluene (90 °C) for 2 h under nitrogen atmosphere, two types of cyclotrimerization products **e** (**1e–2e**) and **f** (**1f–3f**) were formed. The structures of **1e** and **3f**·CH_2Cl_2 are illustrated in Fig. 5, taking as examples. The reaction of $Ru_3(CO)_{12}$ with **4** or **5** afforded, however, no cyclotrimerization products in the same reaction conditions and even extended the reaction time. M. Kawatsura also isolated the alkyne cyclotrimerization products using $Ru_3(CO)_{12}$ as catalyst.[11c]

Step-wise conversion from ynones to final products

To clarify the formation process of the products at each step, the reaction of $Ru_3(CO)_{12}$ with ynones **1–5** were studied in detail and monitored by TLC technique. It was observed that the triruthenium clusters **1a–5a** are unstable, decomposing slowly in toluene. The mixing of **1a–5a** with $Ru_3(CO)_{12}$ in toluene did not give any new ruthenium clusters. By adding the corresponding 1,3-ynones **1–3** in the clusters **1a–3a** in toluene at 90 °C, ruthenoles **b** (**1b–3b**) and **c** (**1c–3c**) were detected. If **4** was added in **4a** in toluene, three ruthenoles **4b**, **4c** and **4d** were found. However, the addition of **5** in **5a** in toluene only **5c** was monitored. Compared with our previous work,[23] no corresponding tetraruthenium clusters were detected in the reaction, however. It is possible that the corresponding tetraruthenium clusters is extremely unstable in the reaction system and cannot be found. The formation of the diverse ruthenoles through reaction of the triruthenium clusters **a** with the corresponding 1,3-ynones justify that the triruthenium cluster **a** is the key intermediates in the generation of ruthenoles.

Then reactions of the ruthenoles with the corresponding ynones were studied to explore how the cyclotrimerization products **e** and **f** were formed. It was found that **e** (**1e–2e**) was detected when ruthenoles **1c** and **2c** were mixed with **1** and **2**, respectively, in toluene at 90 °C. The cyclotrimerization products **1f–3f** were found in the reaction of ruthenoles **1b–3b** with the corresponding **1–3**, respectively. Therefore, we believed that ruthenoles are intermediates during the formation of the cyclotrimerization products.

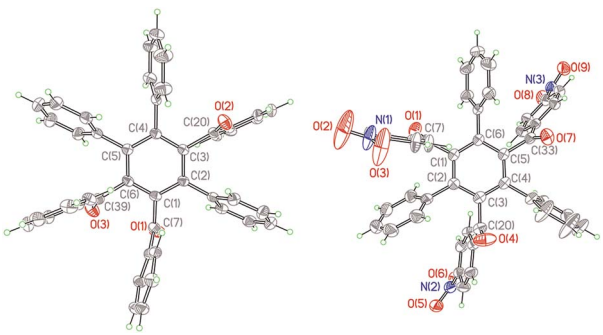

Fig. 5 ORTEP view of cluster **1e** (left) and **3f**·CH_2Cl_2 (right) showing 50% ellipsoids (solvent molecules have been omitted for clarity). Selected bond lengths (Å) and bond angles (°): **1e** (the left): C1–C2 = 1.403(3), C2–C3 = 1.405(2), C3–C4 = 1.400(2), C4–C5 = 1.409(3), C5–C6 = 1.403(3), C1–C6 = 1.398(2), C1–C7 = 1.519(3), C3–C20 = 1.516(3), C6–C39 = 1.513(3), C7–O1 = 1.220(2), C20–O2 = 1.222(3), C39–O3 = 1.222(3). **3f**·CH_2Cl_2 (the right): C1–C2 = 1.399(5), C2–C3 = 1.399(6), C3–C4 = 1.397(4), C4–C5 = 1.398(5), C5–C6 = 1.402(6), C1–C6 = 1.399(4), C1–C7 = 1.507(6), C3–C20 = 1.512(6), C5–C33 = 1.505(4), C7–O1 = 1.217(5), C20–O4 = 1.208(5), C33–O = 1.215(4).

The electronic effect of substituents on the acetylene cyclotrimerization has been reported by T. Takahashi.[27] He found that acetylenes with electron-withdrawing groups (CN, $CONMe_2$ or COPh) could be used for cycloaddition reaction, and unactivated alkynes such as 4-octyne did not give the desired benzene derivatives even at higher temperature.[27] According to the explanation of T. Takahashi, 1,3-diphenylprop-2-yn-1-one is an electron-withdrawing group activated alkyne, so it is feasible that the reaction of **1** with the corresponding ruthenole can afford the cyclotrimerization products **1e** and **1f**. Therefore, it is easier that **2e**, **2f** and **3f** can be produced in the similar reactions. Compound **4** is a derivative of **1** with a strong electron-donating group in the phenyl ring, which weakens the reactivity of **4** in the cyclotrimerization reaction. However, an electron-donating group in the phenyl ring of **1** favors the formation of ruthenole **d**, which can explain the formation of **4d** and a similar compound we reported previously.[23] An *ortho*-acetyl group in the phenyl ring of **5** has certain electron-withdrawing ability, but its larger steric hindrance results in the forming of **5c** as the unique ruthenole in the reaction of **5a** with **5**, and this strong steric effect further prevents the formation of cyclotrimerization products.

Experimental

Materials and equipment

All reactions and manipulations were performed using standard Schlenk line techniques under dry nitrogen. $Ru_3(CO)_{12}$ and the 1,3-ynones were synthesized according to the literature procedure.[28] Solvents were purified, dried and distilled under nitrogen atmosphere prior to use. FT-IR spectra were recorded on a Bruker Tensor 27 Fourier-transform spectrometer. ^1H and $^{13}C\{1H\}$ NMR spectra were performed on a Bruker Avance 400 MHz spectrometer unless indicated. ESI was recorded on a Thermo DecaMax (LC-MS) mass spectrometer with an ion-trap mass detector. While high-resolution mass spectra were recorded in ESI mode on a Waters UPLC-Q-TOF mass spectrometer. The structural measurements of single crystals were carried out with a Bruker SMART APEX-II CCD detector.

Synthesis

1,3-diphenylprop-2-yn-1-one (**1**), 1-(2-chloro-phenyl)-3-phenylprop-2-yn-1-one (**2**), 1-(4-nitro-phenyl)-3-phenylprop-2-yn-1-one (**3**), 1-(2-amino-phenyl)-3-phenylprop-2-yn-1-one (**4**) and 2-(3-phenylpropioloyl)phenylacetate (**5**) were used to react with $Ru_3(CO)_{12}$. Since the reaction processes are similar, the reaction procedure of **1** with $Ru_3(CO)_{12}$ was taken as an example. Both **1** (0.1856 g, 0.9 mmol) and $Ru_3(CO)_{12}$ (0.1918 g, 0.3 mmol) were added in 15 mL toluene and heated at 90 °C for 0.5 h, during which the color of the reaction solution gradually changed from orange to red-brown. The solvent was removed and the residue was chromatographed (the chromatographic column is of 305 mm length and 32 mm internal diameter) on silica gel with dichloromethane and petroleum ether, five main products were eluted in the sequence of **1a**, **1b**, **1c**, **1e** and **1f**, with the eluent dichloromethane/petroleum ether being (v/v) 1 : 5, 3 : 5, 1 : 1, 5 : 3 and 3 : 1, respectively. And then the products were recrystallized by dichloromethane and hexane.

$[Ru_3(CO)_9(\mu\text{-}CO)_2\{\mu_3\text{-}\eta^1\text{:}\eta^2\text{:}\eta^1\text{-}(Ph)C(O)CC(Ph)\}]$ (1a). Yield: 12%. FT-IR (KBr, cm^{-1}): 2923 vs, 2854 s, 2104 s, 2057 vs, 2002 s, 1882 m, 1461 w. ^1H NMR (400 MHz, $CDCl_3$) δ 7.62–7.64 (t, 2H, C_6H_5), 7.29–7.33 (m, 1H, C_6H_5), 7.20–7.24 (t, 2H, C_6H_5), 6.89–6.99 (m, 3H, C_6H_5), 6.82–6.84 (m, 2H, C_6H_5). $^{13}C\{1H\}$ NMR (101 MHz, $CDCl_3$) δ 195.8, 176.4 (CO), 162.6, 148.4 (C≡C), 132.8, 132.3, 129.9, 128.6, 128.3, 128.2, 127.7 (C_6H_5). MS (*m*/*z*, ESI−) 790.737 (M−). Anal. calcd for $C_{25}H_{10}O_{11}Ru_3$: 790.738.

$[Ru(CO)_3\{\mu_4\text{-}\eta^1\text{:}\eta^2\text{:}\eta^1\text{:}\eta^1\text{-}(PhC(O))CC(Ph)C(PhC(O))C(Ph)Ru(CO)_3\}]$ (1b). Yield: 18%. FT-IR (KBr, cm^{-1}): 3074 m, 3028 m, 2958 w, 2927 w, 2858 w, 2090 vs, 2059 vs, 2023 vs, 1994 vs, 1488 vs. ^1H NMR (400 MHz, $CDCl_3$) δ 7.75–7.79 (t, 3H, C_6H_5), 7.27–7.49 (m, 6H, C_6H_5), 7.11–7.15 (m, 1H, C_6H_5), 6.90–7.01 (m, 10H, C_6H_5). $^{13}C\{1H\}$ NMR (101 MHz, $CDCl_3$) δ 196.5, 196.1, 195.8, 194.9, 193.8, 193.4, 192.4, 191.9 (CO), 181.9, 181.2, 145.9, 145.7 (C≡C), 135.5, 134.4, 134.1, 133.9, 133.6, 133.3, 132.8, 132.6, 130.2, 129.8, 129.7, 129.6, 129.1, 128.6, 128.4, 128.0, 127.9, 127.7, 127.6, 123.5 (C_6H_5). MS (*m*/*z*, ESI−) 783.926 (M−). Anal. calcd for $C_{36}H_{20}O_8Ru_2$: 783.925.

$[Ru(CO)_3\{\mu_4\text{-}\eta^1\text{:}\eta^2\text{:}\eta^1\text{:}\eta^1\text{-}(PhC(O))CC(Ph)C(Ph)C(PhC(O))Ru(CO)_3\}\mu\text{-}CO]$ (1c). Yield: 10%. FT-IR (KBr, cm^{-1}): 3026 w, 2923 vs, 2854 s, 2090 vs, 2061 vs, 2029 vs, 2000 vs, 1982 vs, 1448 m. ^1H NMR (400 MHz, $CDCl_3$) δ 7.83–7.85 (d, 3H, C_6H_5), 7.35–7.37 (d, 3H, C_6H_5), 7.26–7.30 (t, 4H, C_6H_5), 7.10–7.12 (d, 4H, C_6H_5), 6.86–6.93 (m, 6H, C_6H_5). $^{13}C\{1H\}$ NMR (101 MHz, $CDCl_3$) δ 197.2, 195.2, 195.0, 193.3 (CO), 169.9 (C≡C), 135.2, 134.2, 132.7, 131.5, 130.9, 130.0, 129.6, 129.4, 129.1, 128.8, 128.7, 128.3, 128.1, 127.8, 123.9, 121.3 (C_6H_5). MS (*m*/*z*, ESI−) 780.923 (M−). Anal. calcd for $C_{36}H_{20}O_8Ru_2$: 780.926.

1,3,4-Triphenyl-2,5,6-tribenzoylbenzene (1e). Yield: 27%. FT-IR (KBr, cm^{-1}): 3058 m, 3026 w, 1668 vs, 1446 m, 1213 vs. ^1H NMR (400 MHz, $CDCl_3$) δ 7.52–7.58 (m, 6H, C_6H_5), 7.26–7.35 (m, 3H, C_6H_5), 7.13–7.21 (m, 9H, C_6H_5), 6.73–7.05 (m, 12H, C_6H_5). $^{13}C\{1H\}$ NMR (101 MHz, $CDCl_3$) δ 198.0, 197.9, 197.3 (CO), 141.3, 140.8, 140.4, 139.2, 139.1, 137.7 (C_6), 137.6, 137.1, 136.9, 136.8, 136.2 (6× $C_6\underline{C}$), 133.0, 132.8, 132.7, 131.0, 130.0, 129.6, 129.5, 129.4, 128.0, 127.8, 127.7, 127.6, 127.3, 127.1, 126.9 (C_6H_5). MS (*m*/*z*, ESI−) 618.219 (M−). Anal. calcd for $C_{45}H_{30}O_3$: 618.219.

1,3,5-Triphenyl-2,4,6-tribenzoylbenzene ($1f\cdot CH_2Cl_2$). Yield: 30%. FT-IR (KBr, cm^{-1}): 3080 m, 3055 m, 3026 m, 1666 vs, 1446 s, 1238 vs. ^1H NMR (400 MHz, $CDCl_3$) δ 7.51 (s, 6H), 7.33 (s, 6H), 7.19 (s, 9H), 6.94 (s, 9H). $^{13}C\{1H\}$ NMR (101 MHz, $CDCl_3$): δ 197.0 (CO), 139.9 (C_6), 137.8, 136.0 (2× $C_6\underline{C}$), 132.9, 130.7, 129.3, 128.0, 127.7, 127.4 (C_6H_5). MS (*m*/*z*, ESI−) 618.219 (M−). Anal. calcd for $C_{45}H_{30}O_3$: 618.219.

$[Ru_3(CO)_9(\mu\text{-}CO)_2\{\mu_3\text{-}\eta^1\text{:}\eta^2\text{:}\eta^1\text{-}(2\text{-}Cl\text{-}PhC(O))CC(Ph)\}]$ (2a). Yield: 5%. FT-IR (KBr, cm^{-1}): 3064 w, 2958 w, 2923 m, 2852 w, 2102 vs, 2071 vs, 2025 vs, 1895 vs, 1645 vs. ^1H NMR (400 MHz, $CDCl_3$) δ 7.32–7.34 (d, 1H, C_6H_4), 6.97–7.18 (m, 6H, C_6H_4, C_6H_5), 6.85–6.87 (d, 2H, C_6H_5). $^{13}C\{1H\}$ NMR (101 MHz, $CDCl_3$) δ 195.7, 177.9 (CO), 162.2, 148.6 (C≡C), 135.1, 133.0, 132.0, 131.1, 131.0, 128.1 (C_6H_4), 127.9, 127.86, 126.4 (C_6H_5). MS (*m*/*z*, ESI−) 824.628 (M−). Anal. calcd for $C_{25}H_9ClO_{11}Ru_3$: 824.699.

$[Ru(CO)_3\{\mu_4\text{-}\eta^1\text{:}\eta^2\text{:}\eta^1\text{:}\eta^1\text{-}(2\text{-ClPhC(O)})CC(Ph)C(2\text{-Cl-PhC(O)})C(Ph)Ru(CO)_3\}]$ (2b). Yield: 20%. FT-IR (KBr, cm^{-1}): 3060 w, 3028 w, 2954 m, 2925 m, 2852 m, 2123 m, 2092 vs, 2061 vs, 2025 vs, 1975 vs, 1664 s. ^1H NMR (400 MHz, $CDCl_3$) δ 7.69–7.70 (d, 1H, C_6H_4), 7.42–7.43 (d, 1H, C_6H_4), 6.97–7.16 (m, 8H, C_6H_4, C_6H_5), 6.66–6.92 (m, 8H, C_6H_4, C_6H_5). $^{13}C\{1H\}$ NMR (101 MHz, $CDCl_3$) δ 196.6, 196.4, 195.7, 194.6, 193.5, 190.7, 179.1, 178.6 (CO), 153.5, 146.0 (C≡C), 140.9, 135.0, 134.8, 134.6, 133.4, 133.2, 133.1, 133.0, 132.8, 132.2, 132.2, 131.4 (C_6H_4), 130.8, 130.6, 128.2, 128.1, 127.7, 127.5, 126.8, 125.7, 124.1, 123.9 (C_6H_4). MS (*m*/*z*, ESI−) 851.862 (M−). Anal. calcd for $C_{36}H_{18}Cl_2O_8Ru_2$: 851.847.

$[Ru(CO)_3\{\mu_4\text{-}\eta^1\text{:}\eta^2\text{:}\eta^1\text{:}\eta^1\text{-}(2\text{-Cl-PhC(O)})CC(Ph)C(Ph)C(2\text{-Cl-Ph-C(O)})Ru(CO)_3\}\mu\text{-CO}]\cdot 1/2C_6H_{14}$ (2c·1/2C_6H_{14}). Yield: 11%. FT-IR (KBr, cm^{-1}): 3060 w, 2956 w, 2923 m, 2854 w, 2090 vs, 2063 vs, 2030 vs, 2000 vs, 1944 vs, 1656 s. ^1H NMR (400 MHz, $CDCl_3$) δ 7.71–7.73 (d, 2H, C_6H_4), 7.15–7.21 (m, 6H, C_6H_4), 7.03–7.15 (d, 4H, C_6H_5), 6.89–6.95 (m, 6H, C_6H_5). $^{13}C\{1H\}$ NMR (101 MHz, $CDCl_3$) δ 197.2, 195.0, 194.4, 193.1 (CO), 168.4 (C≡C), 135.5, 134.0, 133.4, 132.2, 131.6, 131.5 (C_6H_4), 130.2, 128.1, 127.7, 125.8 (C_6H_5). MS (*m*/*z*, ESI−) 851.845 (M−). Anal. calcd for $C_{36}H_{18}Cl_2O_8Ru_2$: 851.847.

1,3,4-Triphenyl-2,5,6-tris(2-chlorobenzoyl)benzene (2e). Yield: 7%. FT-IR (KBr, cm^{-1}): 3057 m, 3026 w, 2956 w, 2925 w, 2852 w, 1666 vs. ^1H NMR (400 MHz, $CDCl_3$) δ 7.46–7.49 (t, 2H, C_6H_4), 7.26–7.28 (d, 1H, C_6H_4), 6.93–7.08 (m, 12H, C_6H_4, C_6H_5), 6.79–6.85 (d, 12H, C_6H_4, C_6H_5). $^{13}C\{1H\}$ NMR (101 MHz, $CDCl_3$) δ 196.6, 196.5, 194.9 (CO), 142.6, 141.2, 141.0, 140.6, 139.4 (C_6), 137.7, 136.8, 136.5, 136.4, 136.1 (6× $C_6\underline{C}$), 133.3, 133.1, 133.0, 132.8, 132.4, 132.3, 132.2, 131.6, 130.8, 130.4 (C_6H_4), 130.1, 129.5, 127.9, 127.7, 127.6, 127.4, 127.1, 127.0, 126.3, 126.0 (C_6H_5). MS (*m*/*z*, ESI−) 722.099 (M−). Anal. calcd for $C_{45}H_{27}Cl_3O_3$: 722.100.

1,3,5-Triphenyl-2,4,6-tris(2-chlorobenzoyl)benzene (2f). Yield: 24%. FT-IR (KBr, cm^{-1}): 3060 m, 2966 w, 2854 w, 1668 vs, 1224 vs. ^1H NMR (400 MHz, $CDCl_3$) δ 7.28–7.30 (d, 3H, C_6H_4), 6.93–7.19 (m, 24H, C_6H_4, C_6H_5). $^{13}C\{1H\}$ NMR (101 MHz, $CDCl_3$) δ 194.5 (CO), 140.8, 139.4, 136.6 (2× $C_6\underline{C}$), 136.3, 133.0, 132.6, 132.0, 130.7 (C_6H_4), 129.9, 127.8, 127.7, 126.9, 126.3 (C_6H_5). MS (*m*/*z*, ESI−) 722.100 (M−). Anal. calcd for $C_{45}H_{27}Cl_3O_3$: 722.100.

$[Ru_3(CO)_9(\mu\text{-}CO)_2\{\mu_3\text{-}\eta^1\text{:}\eta^2\text{:}\eta^1\text{-}(Ph)CC(4\text{-}NO_2\text{-PhC(O)})\}]$ (3a). Yield: 7%. FT-IR (KBr, cm^{-1}): 2923 vs, 2854 s, 2059 m, 2017 m, 1460 m. ^1H NMR (400 MHz, $CDCl_3$) δ 8.05–8.10 (m, 2H, C_6H_4), 7.75–7.77 (d, 2H, C_6H_4), 6.93–6.99 (m, 4H, C_6H_5), 6.78–6.80 (d, 1H, C_6H_5). $^{13}C\{1H\}$ NMR (101 MHz, $CDCl_3$) δ 192.9, 176.2 (CO), 158.6, 148.9 (C≡C), 147.3, 136.6, 130.0, 129.5, 127.8 (C_6H_4), 127.4, 126.8, 126.5, 122.7, 122.1 (C_6H_5), 122.0 (C_6H_4). MS (*m*/*z*, ESI−) 835.724 (M−). Anal. calcd for $C_{25}H_9NO_{13}Ru_3$: 835.723.

$[Ru(CO)_3\{\mu_4\text{-}\eta^1\text{:}\eta^2\text{:}\eta^1\text{:}\eta^1\text{-}(4\text{-}NO_2PhC(O))CC(Ph)C(4\text{-}NO_2\text{-PhC(O)})C(Ph)Ru(CO)_3\}]\cdot C_6H_{14}$ (3b·C_6H_{14}). Yield: 22%. FT-IR (KBr, cm^{-1}): 3105 w, 3076 w, 3055 w, 2098 vs, 2067 vs, 2027 vs, 1975 vs, 1529 vs, 1344 vs. ^1H NMR (400 MHz, $CDCl_3$) δ 8.12–8.21 (m, 8H, C_6H_4), 6.88–7.01 (m, 10H, C_6H_5). $^{13}C\{1H\}$ NMR (101 MHz, $CDCl_3$) δ 196.0, 195.2, 194.7, 194.4, 192.5, 191.2, 179.5, 177.7 (CO), 150.3, 149.9 (C≡C), 145.3, 139.4, 139.0, 133.5, 130.4, 130.2, 129.7, 129.6, 129.1, 128.7 (C_6H_4), 128.5, 128.1, 123.9, 123.5 (C_6H_5), 123.4 (C_6H_4). MS (*m*/*z*, ESI−) 872.910 (M−). Anal. calcd for $C_{36}H_{18}N_2O_{12}Ru_2$: 872.896.

$[Ru(CO)_3\{\mu^4\text{-}\eta^1\text{:}\eta^2\text{:}\eta^1\text{:}\eta^1\text{-}(4\text{-}NO_2\text{-PhC(O)})CC(Ph)C(Ph)C(4\text{-}NO_2Ph\text{-C(O)})Ru(CO)_3\}\mu\text{-CO}]$ (3c). Yield: 19%. FT-IR (KBr, cm^{-1}): 3053 w, 2958 w, 2925 w, 2854 w, 2096 vs, 2063 vs, 2021 vs, 1523 s, 1334 s. ^1H NMR (400 MHz, $CDCl_3$) δ 8.35–8.37 (d, 2H, C_6H_4), 8.22–8.24 (d, 2H, C_6H_4), 8.14–8.19 (t, 2H, C_6H_4), 8.04–8.10 (m, 2H, C_6H_4), 7.84–7.94 (m, 1H, C_6H_5), 7.61–7.72 (m, 2H, C_6H_5), 7.45–7.51 (t, 3H, C_6H_5), 7.14–7.16 (d, 1H, C_6H_5), 6.94–7.09 (m, 3H). $^{13}C\{1H\}$ NMR (101 MHz, $CDCl_3$) δ 195.4, 194.9, 193.8, 192.8, 189.1 (CO), 167.7, 150.1 (C≡C), 149.9, 146.9, 143.1, 139.7, 134.3, 133.5, 131.3, 131.2, 130.7, 130.3 (C_6H_4), 129.4, 129.1, 128.9, 128.7, 128.6, 128.2, 123.9 (C_6H_5), 123.5, 123.4, 121.3 (C_6H_4). MS (*m*/*z*, ESI−) 872.893 (M−). Anal. calcd for $C_{36}H_{18}N_2O_{12}Ru_2$: 872.896.

1,3,5-Triphenyl-2,4,6-tris(4-nitrobenzoyl)benzene·CH_2Cl_2 (3f·CH_2Cl_2). Yield: 16%. FT-IR (KBr, cm^{-1}): 3105 w, 3060 w, 2925 w, 2856 w, 1683 s, 1525 vs, 1346 s. ^1H NMR (400 MHz, $CDCl_3$) δ 8.04–8.08 (t, 6H, C_6H_4), 7.63–7.71 (m, 6H, C_6H_4), 6.91–7.03 (d, 15H, C_6H_5). $^{13}C\{1H\}$ NMR (101 MHz, $CDCl_3$) δ 197.0, 196.8, 194.8 (CO), 150.0, 149.9, 149.8 (C_6H_4), 142.1, 142.0, 141.5, 141.2, 141.0, 139.3 (C_6), 139.2, 135.7, 135.2 (2× $C_6\underline{C}$), 134.9, 130.9, 130.0, 129.9 (C_6H_4), 128.7, 128.1, 127.9, 123.4, 123.2, 123.1 (C_6H_5). MS (*m*/*z*, ESI−) 753.175 (M−). Anal. calcd for $C_{45}H_{27}N_3O_9$: 753.175.

$[Ru_3(CO)_9(\mu\text{-}CO)_2\{\mu_3\text{-}\eta^1\text{:}\eta^2\text{:}\eta^1\text{-}(Ph)CC(2\text{-}NH_2\text{-PhC(O)})\}]$ (4a). Yield: 7%. FT-IR (KBr, cm^{-1}): 2952 vs, 2923 vs, 2854 s, 2073 m, 2046 m, 2011 m, 1460 m. ^1H NMR (400 MHz, $CDCl_3$) δ 7.52–7.54 (d, 2H, C_6H_4), 6.97–7.03 (m, 5H, C_6H_5), 6.84–6.89 (t, 2H, C_6H_4), 6.45–6.47 (d, 2H, NH_2). $^{13}C\{1H\}$ NMR (101 MHz, $CDCl_3$) δ 194.5, 175.9 (CO), 164.5 (C_6H_4), 150.8, 148.5 (C≡C), 132.5, 128.1 (C_6H_4), 128.0, 127.7 (C_6H_5), 113.9 (C_6H_4). MS (*m*/*z*, ESI−) 805.673 (M−). Anal. calcd for $C_{25}H_{11}NO_{11}Ru_3$: 805.749.

$[Ru(CO)_3\{\mu_4\text{-}\eta^1\text{:}\eta^2\text{:}\eta^1\text{:}\eta^1\text{-}(2\text{-}NH_2PhC(O))CC(Ph)C(2\text{-}NH_2\text{-PhC(O)})C(Ph)Ru(CO)_3\}]$ (4b). Yield: 29%. FT-IR (KBr, cm^{-1}): 3483 m, 3340 m, 3057 w, 2923 s, 2854 m, 2088 vs, 2059 vs, 2021 vs, 2000 vs, 1973 vs, 1581 s. ^1H NMR (400 MHz, $CDCl_3$) δ 7.54–7.62 (dd, 2H, C_6H_4), 6.88–7.06 (m, 12H, C_6H_4, C_6H_5), 6.51–6.55 (t, 1H, C_6H_4), 6.32–6.41 (m, 3H, C_6H_4), 5.94–5.97 (d, 4H, NH_2). $^{13}C\{1H\}$ NMR (101 MHz, $CDCl_3$) δ 199.3, 196.6, 196.2, 195.4, 194.1, 193.5, 184.5, 175.1 (CO), 150.5, 150.4 (C_6H_4), 146.3, 135.4 (C≡C), 134.8, 134.4, 134.3, 133.9, 133.8, 130.1, 128.7, 128.1 (C_6H_4), 127.8, 127.4, 127.3, 123.2, 117.4, 117.0, 115.9 (C_6H_5), 114.8 (C_6H_4). MS (*m*/*z*, ESI−) 812.948 (M−). Anal. calcd for $C_{36}H_{22}N_2O_8Ru_2$: 812.948.

$[Ru(CO)_3\{\mu_4\text{-}\eta^1\text{:}\eta^2\text{:}\eta^1\text{:}\eta^1\text{-}(2\text{-}NH_2\text{-PhC(O)})CC(Ph)C(Ph)C(2\text{-}NH_2Ph\text{-C(O)})Ru(CO)_3\}\mu\text{-CO}]$ (4c). Yield: 15%. FT-IR (KBr, cm^{-1}): 2954 s, 2923 vs, 2854 s, 2057 s, 2003 s, 1961 m, 1593 m. ^1H NMR (400 MHz, $CDCl_3$) δ 7.75–7.89 (dd, 2H, C_6H_4), 7.28–7.57 (m, 12H, C_6H_4, C_6H_5), 6.96–7.12 (m, 4H, C_6H_4), 6.70–6.91 (m, 4H, NH_2). $^{13}C\{1H\}$ NMR (101 MHz, $CDCl_3$) δ 186.5 (CO), 153.2 (C_6H_4), 136.1, 135.4 (C≡C), 134.8, 128.5, 125.1, 120.7 (C_6H_4), 118.5, 115.9, 112.0 (C_6H_5), 111.5 (C_6H_4). MS (*m*/*z*, ESI−) 812.948 (M−). Anal. calcd for $C_{36}H_{22}N_2O_8Ru_2$: 812.948.

$[Ru(CO)_3\{\mu_4\text{-}\eta^1\text{:}\eta^2\text{:}\eta^1\text{:}\eta^1\text{-}(Ph)CC(2\text{-}NH_2PhC(O))C(2\text{-}NH_2\text{-PhC(O)})C(Ph)Ru(CO)_3\}]\cdot 3/4CH_2Cl_2$ (4d·3/4CH_2Cl_2). Yield: 23%. FT-IR (KBr, cm^{-1}): 3475 w, 3348 w, 2952 s, 2923 vs, 2854 s, 2088 vs, 2057 vs, 2019 vs, 1969 vs, 1639 m. ^1H NMR

(400 MHz, $CDCl_3$) δ 7.60–7.87 (m, 3H, C_6H_4), 7.21–7.41 (m, 5H, C_6H_4, C_6H_5), 6.94–7.12 (m, 8H, C_6H_4, C_6H_5), 6.83–6.86 (t, 1H, C_6H_4), 6.68–6.71 (t, 1H, C_6H_4), 6.01–6.32 (m, 4H, NH_2). $^{13}C\{1H\}$ NMR (101 MHz, $CDCl_3$) δ 197.8, 196.4, 194.4, 193.8, 192.7, 191.7, 180.6 (CO), 151.0, 150.4 (C_6H_4), 146.1, 143.0 (C≡C), 135.3, 134.6, 134.5, 134.3, 133.2, 131.4, 131.0, 130.1 (C_6H_4), 129.0, 128.9, 128.3, 127.6, 127.3, 123.2, 117.3, 116.3 (C_6H_5), 115.9, 115.3 (C_6H_4). MS (*m*/*z*, ESI−) 815.947 (M−). Anal. calcd for $C_{36}H_{22}N_2O_8Ru_2$: 815.947.

$[Ru_3(CO)_9(\mu\text{-}CO)_2\{\mu_3\text{-}\eta^1\text{:}\eta^2\text{:}\eta^1\text{-}(2\text{-}CH_3COO\text{-}PhC(O))CC(Ph)\}]$ (5a). Yield: 10%. FT-IR (KBr, cm^{-1}): 3058 w, 3030 w, 2925 w, 2854 w, 2104 m, 2071 vs, 2056 vs, 2017 vs, 1878 m, 1760 m. ^1H NMR (400 MHz, $CDCl_3$) δ 7.27–7.30 (m, 2H, C_6H_4), 7.00–7.05 (m, 3H, C_6H_4, C_6H_5), 6.87–6.96 (m, 4H, C_6H_5), 2.23 (s, 3H, CH_3). $^{13}C\{1H\}$ NMR (101 MHz, $CDCl_3$) δ 194.8, 174.7, 169.6 (CO), 166.5 (C_6H_4), 150.8, 148.2 (C≡C), 133.5, 131.7, 128.3, 127.9 (C_6H_4), 127.7, 125.9, 125.6 (C_6H_5), 124.4 (C_6H_4), 21.0 (CH_3). MS (*m*/*z*, ESI−) 846.728 (M−). Anal. calcd for $C_{27}H_{12}O_{13}Ru_3$: 846.742.

$[Ru(CO)_3\{\mu_4\text{-}\eta^1\text{:}\eta^2\text{:}\eta^1\text{:}\eta^1\text{-}(2\text{-}CH_3COO\text{-}PhC(O))CC(Ph)C(Ph)C(2\text{-}CH_3COOPh\text{-}C(O))Ru(CO)_3\}\mu\text{-}CO]\cdot CH_2Cl_2$ (5c·CH_2Cl_2). Yield: 29%. FT-IR (KBr, cm^{-1}): 3060 w, 3030 w, 2927 w, 2854 w, 2092 vs, 2063 vs, 2025 vs, 1975 vs, 1770 s, 1118 vs. ^1H NMR (400 MHz, $CDCl_3$) δ 7.63–7.85 (m, 3H, C_6H_4), 7.33–7.44 (m, 3H, C_6H_4), 7.10–7.24 (m, 2H, C_6H_4), 6.85–7.04 (m, 10H, C_6H_5), 2.21–2.29 (t, 6H, CH_3). $^{13}C\{1H\}$ NMR (101 MHz, $CDCl_3$) δ 196.3, 195.8, 195.7, 195.0, 194.8, 194.3, 193.4, 189.9, 180.4 (CO), 169.6, 169.1 (C_6H_4), 149.8, 149.8, 145.8, 134.2 (C≡C), 134.1, 133.9, 133.3, 133.1, 132.7, 132.5, 132.2, 131.9 (C_6H_4), 131.4, 130.0, 128.6, 128.4, 128.2, 128.1, 127.8, 127.6, 127.4, 125.7, 125.0, 124.9 (C_6H_5), 124.5, 123.9 (C_6H_4), 20.9 (CH_3). MS (*m*/*z*, ESI−) 899.931 (M−). Anal. calcd for $C_{40}H_{24}O_{12}Ru_2$: 899.935.

Crystallography

X-ray structural measurements were carried out with a Bruker SMART APEX-II CCD detector using graphite monochromated MoKα radiation ($\lambda = 0.71073$). The data were collected by the ω–2θ scan mode, and absorption correction was applied by using Multi-Scan. The structure was solved by direct methods (SHELXS-97) and refined by full-matrix least squares against F2 using SHELXL-97 software.[29] Non-hydrogen atoms were refined with anisotropic thermal parameters. All hydrogen atoms were geometrically fixed and refined using a riding model.

The single crystals of compounds **1a**, **1b**, **1e**, **1f**, **2a**, **2c**, **3b**, **3f**, **4b**, **4d**, **5a** and **5c** suitable for single crystal X-ray diffraction were successfully grown up from slow evaporation of their dichloromethane/hexane solutions at 4 °C. Relevant crystallographic data were given in Table S1 in the ESI.† Crystallographic data for the structural analysis have been deposited with the Cambridge Crystallographic Data Centre: 1553521 (**1a**), 1553523 (**1b**), 1553526 (**1e**), 1553527 (**1f**), 1553511 (**2a**), 1553512 (**2c**), 1545197 (**3b**), 1545199 (**3f**), 1553513 (**4b**), 1553516 (**4d**), 1553504 (**5a**) and 1553509 (**5c**).†

Conclusions

We isolated a series of new ruthenium clusters and cyclotrimerization products by investigating reactions of five 1,3-diphenylprop-2-yn-1-one derivatives with $Ru_3(CO)_{12}$. The activation of the 1,3-ynones and the transformation of the cluster skeletons demonstrated that the triruthenium clusters and ruthenoles are important intermediates during the formation of the final products. More importantly, the substituents in the phenyl ring of 1,3-diphenylprop-2-yn-1-one exerted great effects on the reaction pathways during the transformation reactions. We revealed that the product distribution is dependent strongly on both the electronic and steric effects of the substituents on the acetylenic ketones. This discovery allows us to control the direction of the reaction by adjusting the substituents in the phenyl ring of 1,3-diphenylprop-2-yn-1-one. Moreover, further reactions between ruthenoles and the corresponding alkyne ketones proceed if a group can activate the carbon–carbon triple bond of an alkyne ketone, it brings us a new idea about applications of ruthenoles in the field of organic synthesis.

Conflicts of interest

There are no conflicts to declare.

Acknowledgements

This work is supported by the National Natural Science Foundation of China (21401124, 21171112).

Notes and references

1 (*a*) T. C. Johnson, W. G. Totty and M. Wills, *Org. Lett.*, 2012, **14**, 5230; (*b*) A. Lennartson, A. Lundin, K. Boerjesson, V. Gray and K. Moth-Poulsen, *Dalton Trans.*, 2016, **45**, 8740; (*c*) M. Chen, M. Zhang, B. Xiong, Z. Tan, W. Lv and H. Jiang, *Org. Lett.*, 2014, **16**, 6028; (*d*) D. C. Schmitt, J. Lee, A. R. Dechert-Schmitt, E. Yamaguchi and M. J. Krische, *Chem. Commun.*, 2013, **49**, 6096; (*e*) L. Wang and L. Ackermann, *Chem. Commun.*, 2014, **50**, 1083; (*f*) F. Xie, M. Zhang, H. Jiang, M. Chen, W. Lv, A. Zheng and X. Jian, *Green Chem.*, 2015, **17**, 279; (*g*) J. A. Cabeza, I. del Rio, E. Perez-Carreno and V. Pruneda, *Organometallics*, 2011, **30**, 1148.

2 (*a*) J. Liu, C. Kubis, R. Franke, R. Jackstell and M. Beller, *ACS Catal.*, 2016, **6**, 907; (*b*) Z. Fan, J. Ni and A. Zhang, *J. Am. Chem. Soc.*, 2016, **138**, 8470; (*c*) Y. Yuki, K. Takahashi, Y. Tanaka and K. Nozaki, *J. Am. Chem. Soc.*, 2013, **135**, 17393; (*d*) N. Armanino, M. Lafrance and E. M. Carreira, *Org. Lett.*, 2014, **16**, 572; (*e*) S. T. Tan, J. W. Kee and W. Y. Fan, *Organometallics*, 2011, **30**, 4008; (*f*) X. Guo and C. J. Li, *Org. Lett.*, 2011, **13**, 4977.

3 L. Wu, I. Fleischer, R. Jackstell and M. Beller, *J. Am. Chem. Soc.*, 2013, **135**, 3989.

4 (*a*) I. Profir, M. Beller and I. Fleischer, *Org. Biomol. Chem.*, 2014, **12**, 6972; (*b*) W. J. Park, C. H. Lee, D. S. Kim and C. H. Jun, *Chem. Commun.*, 2015, **51**, 14667; (*c*) D. S. Kim, W. J. Park, C. H. Lee and C. H. Jun, *J. Org. Chem.*, 2014, **79**, 12191; (*d*) M. Nishiumi, H. Miura, K. Wada, S. Hosokawa and M. Inoue, *Adv. Synth. Catal.*, 2010, **352**, 3045.

5 W. Li, X. Huang and J. You, *Org. Lett.*, 2016, **18**, 666.

6 (*a*) A. Saxena, F. Perez and M. J. Krische, *Angew. Chem., Int. Ed.*, 2016, **55**, 1493; (*b*) B. Groell, M. Schnuerch and M. D. Mihovilovic, *J. Org. Chem.*, 2012, **77**, 4432; (*c*) A. Saxena, F. Perez and M. J. Krische, *J. Am. Chem. Soc.*, 2015, **137**, 5883; (*d*) M. Kawatsura, M. Yamamoto, J. Namioka, K. Kajita, T. Hirakawa and T. Itoh, *Org. Lett.*, 2011, **13**, 1001.

7 (*a*) B. Y. Park, T. Luong, H. Sato and M. J. Krische, *J. Am. Chem. Soc.*, 2015, **137**, 7652; (*b*) T. C. Johnson, W. J. Totty and M. Wills, *Org. Lett.*, 2012, **14**, 5230.

8 (*a*) K. Takahashi, M. Yamashita and K. Nozaki, *J. Am. Chem. Soc.*, 2012, **134**, 18746; (*b*) E. L. McInturff, J. Mowat, A. R. Waldeck and M. J. Krische, *J. Am. Chem. Soc.*, 2013, **135**, 17230; (*c*) B. Li, Y. Park and S. Chang, *J. Am. Chem. Soc.*, 2014, **136**, 1125.

9 (*a*) B. Y. Park, T. P. Montgomery, H. J. Garza and M. J. Krische, *J. Am. Chem. Soc.*, 2013, **135**, 16320; (*b*) S. E. Denmark and Z. D. Matesich, *J. Org. Chem.*, 2014, **79**, 5970.

10 (*a*) D. Chen, C. Zhang, S. Xu, H. Song and B. Wang, *Organometallics*, 2011, **30**, 676; (*b*) C. Zhang, B. Li, H. Song, S. Xu and B. Wang, *Organometallics*, 2011, **30**, 3029; (*c*) W. K. Tsui, L. H. Chung, W. H. Tsang, C. F. Yeung, C. H. Chiu, H. S. Lo and C. Y. Wong, *Organometallics*, 2015, **34**, 1005; (*d*) B. F. G. Johnson, J. M. Matters, P. E. Gaede, S. L. Ingham, N. Choi, M. Mcpartlin and M. A. Pearsall, *Dalton Trans.*, 1997, **18**, 3251; (*e*) M. I. Bruce, M. L. Cole, R. S. C. Fung, C. M. Forsyth, P. C. Junk and K. Konstas, *Dalton Trans.*, 2008, **31**, 4118.

11 (*a*) H. Sato, M. Bender, W. J. Chen and M. J. Krische, *J. Am. Chem. Soc.*, 2016, **138**, 16244; (*b*) J. P. Hopewell, J. E. D. Martins, T. C. Johnson, J. Godfrey and M. Wills, *Org. Biomol. Chem.*, 2012, **10**, 134; (*c*) M. Kawatsura, M. Yamamoto, J. Namioka, K. Kajita, T. Hirakawa and T. Itoh, *Org. Lett.*, 2011, **13**, 1001.

12 S. V. Osintseva, F. M. Dolgushin, N. A. Shtel'tser, P. V. Petrovskii, A. S. Peregudov, A. Z. Kreindlin and M. Y. Antipin, *Organometallics*, 2010, **29**, 1012.

13 C. S. Chen, Y. F. Lin and W. Y. Yeh, *Chem.–Eur. J.*, 2014, **20**, 936.

14 (*a*) M. Krempe, R. Lippert, F. Hampel, I. Ivanovic-Burmazovic, N. Jux and R. R. Tykwinski, *Angew. Chem., Int. Ed.*, 2016, **55**, 14802; (*b*) C. Cesari, L. Sambri, S. Zacchini, V. Zanotti and R. Mazzoni, *Organometallics*, 2014, **33**, 2814; (*c*) H. Masai, J. Terao, S. Seki, S. Nakashima, M. Kiguchi, K. Okoshi, T. Fujihara and Y. Tsuji, *J. Am. Chem. Soc.*, 2014, **136**, 1742; (*d*) O. F. Koentjoro, P. J. Low, R. Rousseau, C. Nervi, D. S. Yufit, J. A. K. Howard and K. A. Udachin, *Organometallics*, 2005, **24**, 1284.

15 P. J. Low, *J. Cluster Sci.*, 2008, **19**, 5.

16 G. Gervasio, D. Marabello, E. Sappa and A. Secco, *J. Organomet. Chem.*, 2005, **690**, 1594.

17 M. Hernandez-Sandoval, G. Sanchez-Cabrera, M. J. Rosales-Hoz, M. A. Leyva, V. Salazar, J. G. Alvarado-Rodriguez and F. J. Zuno-Cruz, *Polyhedron*, 2013, **52**, 170.

18 P. Mathur, D. K. Rai, R. K. Joshi, B. Jha and S. M. Mobin, *Organometallics*, 2014, **33**, 3857.

19 (*a*) S. V. Osintseva, F. M. Dolgushin, N. A. Shtel'tser, P. V. Petrovskii, A. Z. Kreindlin, L. V. Rybin and M. Y. Antipin, *Organometallics*, 2005, **24**, 2279; (*b*) W. K. Tsui, L. H. Chung, W. H. Tsang, C. F. Yeung, C. H. Chiu, H. S. Lo and C. Y. Wong, *Organometallics*, 2015, **34**, 1005.

20 (*a*) B. H. Xu, G. Kehr, R. Froehlich, B. Wibbeling, B. Schirmer, S. Grimme and G. Erker, *Angew. Chem., Int. Ed.*, 2011, **50**, 7183; (*b*) W. P. Unsworth, J. D. Cuthbertson and R. J. K. Taylor, *Org. Lett.*, 2013, **15**, 3306; (*c*) J. Shen, G. Cheng and X. Cui, *Chem. Commun.*, 2013, **49**, 10641; (*d*) J. D. Kirkham, S. J. Edeson, S. Stokes and J. P. A. Harrity, *Org. Lett.*, 2012, **14**, 5354; (*e*) M. Yoshida, K. Saito, Y. Fujino and T. Doi, *Chem. Commun.*, 2012, **48**, 11796; (*f*) N. Arai, H. Satoh, N. Utsumi, K. Murata, K. Tsutsumi and T. Ohkuma, *Org. Lett.*, 2013, **15**, 3030.

21 G. G. Melikyan, R. Davis, B. Anker, D. Meron and K. Duncan, *Organometallics*, 2016, **35**, 4060.

22 (*a*) S. V. Osintseva, F. M. Dolgushin, N. A. Shtel'tser, P. V. Petrovskii, A. S. Peregudov, A. Z. Kreindlin and M. Y. Antipin, *Organometallics*, 2010, **29**, 1012; (*b*) C. S. Chen, Y. F. Lin and W. Y. Yeh, *Chem.–Eur. J.*, 2014, **20**, 936.

23 J. Yang, W. Zhang, G. Zhang and Z. Gao, *J. Organomet. Chem.*, 2015, **799**, 166.

24 D. Delgado, E. Hernandez, A. Martin and M. Menacho, *Organometallics*, 2006, **25**, 2960.

25 X. M. Chen and J. W. Cai, in *Single-Crystal Structural Analysis-Principles and Practices*, Science China Press, Beijing, China, 2nd edn, 2004, p. 114.

26 (*a*) A. J. Arce, P. Arrojo, A. J. Deeming and Y. De Sanctis, *Dalton Trans.*, 1992, **15**, 2423; (*b*) A. J. Arce, R. Machado, C. Rivas, Y. De Sanctis and A. J. Deeming, *J. Organomet. Chem.*, 1991, **419**, 63.

27 T. Takahashi, Z. Xi, A. Yamazaki, Y. Liu, K. Nakajima and M. Kotora, *J. Am. Chem. Soc.*, 1998, **120**, 1672.

28 B. Yu, H. Sun, Z. Xie, G. Zhang, L. Xu, W. Zhang and Z. Gao, *Org. Lett.*, 2015, **17**, 3298.

29 G. M. Sheldrick, *Acta Crystallogr., Sect. A: Found. Crystallogr.*, 2008, **64**, 112.